DOE/JPL/954853-4

ARRAY AUTOMATED ASSEMBLY. PHASE 2

Quarterly Report Ending September 30, 1978

By
William E. Taylor
William Kimberly
Nick Mardesich
Angel Pepe

October 1978

Work Performed Under Contract No. NAS-7-100-954853

Spectrolab, Incorporated
Sylmar, California

U.S. Department of Energy

Solar Energy

DISCLAIMER

NOTICE

DOE/JPL/954853-4
Distribution Category UC-63b

ARRAY AUTOMATED ASSEMBLY

PHASE 2

Quarterly Report
For the Quarter Ending September 30, 1978

Prepared by:
William E. Taylor, William Kimberly
Nick Mardesich, and Angel Pepe

October 1978

JPL Contract No. 954853

SPECTROLAB INC.
12500 Gladstone Avenue
Sylmar, California 91342

The JPL Low-Cost Silicon Solar Array Project is sponsored by the U. S. Department of Energy and forms part of the Solar Photovoltaic Conversion Program to initiate a major effort toward the development of low-cost solar arrays. This work was performed for the Jet Propulsion Laboratory, California Institute of Technology by agreement by NASA and DOE.

TABLE OF CONTENTS

1.0 SUMMARY STATEMENT

Problems with excessive junction shunting previously reported were found to be associated with a malfunction discovered in one of the printers. Aluminum contamination of the front surface and junction edge were also identified as sources of shunting, as was damage to the tetrahedral peaks during handling of diffused wafers.

Additional compositional variations of titania precipitated and baria-magnesia borosilicate glasses were prepared to improve fusion and maturation characteristics. An intensive effort was made to integrate the diffusion mask process into the process sequence. This attempt has been unsuccessful. All cells fabricated have had very low output attributable primarily to low shunt resistance.

Alcoa 1401 and AMPAL (Atomized Metal Powder, Inc.) aluminum powders were tested as the base for making screen printing pastes for back surface P+ contacts. Time-temperature firing matrix experiments showed that optimum conditions were different for the two different pastes: 850^{o}C and 20 seconds for the paste based on Alcoa 1401 powder and 825^{o}C for 30 seconds for the paste based on the AMPAL powder.

Additional peel strength data on protective coating materials were gathered. The effect of exposure to a swelling solvent on coating layers was added as a test of adhesive bonding to the substrate and the effectiveness of primer coupling agents. The preliminary tests indicate ability to discriminate between different primers used with RTV-type silicon coatings.

Evaluation of currently available processes for AR coating glass has led to the conclusion that these processes are not adequately developed for the treatment of large panes of glass and are probably not suitable for mass production purposes.

2.0 INTRODUCTION

This Interim Technical Progress Report covers the period July 1, 1978 to September 30, 1978. The scope of the contract covers the investigation of technology readiness of a proposed process sequence for the low cost fabrication of photovoltaic modules as part of the Phase 2 of the Array Automated Assembly Task, Low Cost Silicon Solar Array Project.

2.1 TECHNICAL OVERVIEW OF CELL DESIGN AND PROCESS SEQUENCE

The cell design and process sequence as modified by work performed to date are shown in Table 2-1. Steps where major modifications have been made in the process sequence are indicated by asterisks. Cross sectional views of the originally proposed and modified structures are shown in Figure 2.1.

The originally proposed design included shaped cells in order to achieve the goal of 12-13% module efficiency. During the first quarter an analysis of cost trade-offs showed that the optimum degree of partial shaping from cylindrical crystals would be a circle with small flats, leading to significant unoccupied interstitial areas in the module. For process verification purposes we have resolved to use square cells shaped from Czochralski crystals in anticipation of the eventual availability of square or rectangular sheet material.

Spectrolab's plan includes the use of texturized surfaces, conforming with the conclusions of the Phase 1 studies. The texturizing process is adequate, under some circumstances to also remove saw damaged surface material.

Table 2.1

CELL DESIGN AND PROCESS SEQUENCE

Revised August 26, 1978

1. Design:

   Shaped, size 5.38 cm square (29 cm^2)
   Texturized surface
   N+ junction diffusion
   P+ back surface field
   Printed contact metallization
   Wraparound contacts
   η_c = 15% (28°C, 100 mW/cm^2)

2. Process Sequence:

   1) Surface preparation
   2)* Diffusion mask process deleted
   3) Apply front polymer dopant
   4) Diffusion
   5) Print aluminum back
   5a)*Fire aluminum back
   5b)*Strip diffusion oxide and clean Al back
   6)* Edge Clean-up
   7) Print back isolation dielectric
   8) Fire back isolation dielectric
   9) Print contact pad over dielectric
   10) Print front grid pattern and wraparound conductors
   11) Fire contact pad, grid pattern and wraparound conductors
   11a)*Apply tin solder pad on aluminum back
   11b)*AR coat
   12) Test cells

*Steps where major modifications from original proposal have been introduced.

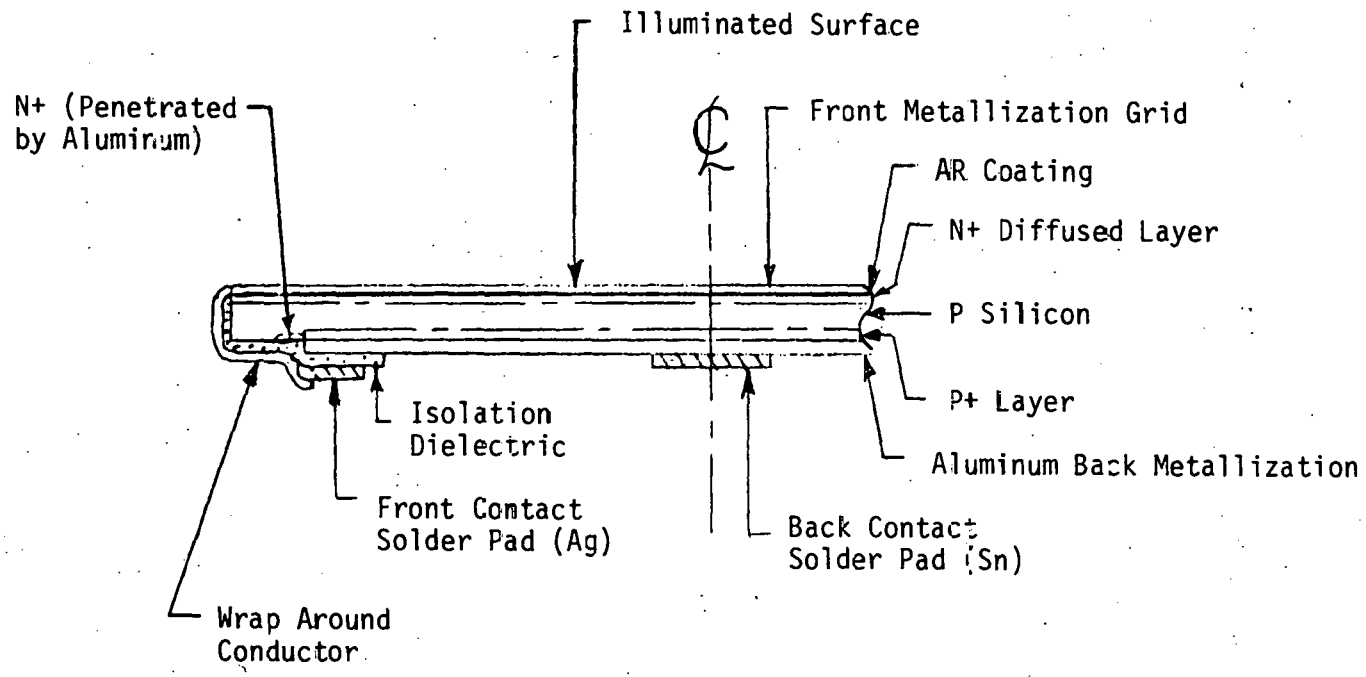

1b. Modified as of 8-26-78

Figure 2.1

The cell design included a P+ back field obtained from a printed aluminum source. The N+ diffusion was to be obtained from a phosphorus doped polymer source. An innovative approach to the junction formation process was included; namely, the use of a prefired diffusion masking dielectric on the edge of the cell. This was intended to permit the codiffusion of the N+ and P+ regions without the need for an edge etch. A number of glass formulations have been tested with positive results as to a diffusion barrier; however, attempts to integrate this process into the total process sequence have not been successful. All attempts to fabricate cells using these materials resulted in low output cells due to severe junction shunting. In the interest of proceeding with verification of other process steps we have decided to set aside the diffusion mask process for the present. This will necessitate the introduction of an edge clean-up step. Edge grinding and edge etching by either wet chemistry or plasma techniques are under consideration.

A further use for the edge masking dielectric was to be as an insulation layer for wraparound contacts. Elimination of the diffusion mask process will require extension of the back isolation dielectric around the edge of the cell to provide this function.

A spin-on diffusion source, Emulsitone N-250 has been selected. Spray-on and contact transfer application techniques have been evaluated and found to be satisfactory. As a further innovation, it was originally proposed that the diffusion oxide not be removed, but retained to serve as an antireflection coating. It has been determined that retention of the diffusion oxide results in excess series resistance, and hence its retention as an AR coating is not feasible. Cofiring of the aluminum back field during diffusion was found to be unsatisfactory. However it was observed that the printed aluminum can be fired through a diffused layer with satisfactory results. This permits the use of a separate firing step

Table 2.2

MODULE DESIGN AND PROCESS SEQUENCE

Revised August 26, 1978

1. Design

   Size 60 x 120 cm (2 x 4 ft)
   Tempered glass superstrate
   Cells attached by polymeric adhesive
   Preformed circuit interconnects
   3 mil polymeric conformal coating
   Aluminum extrusion frame
   η_m = 12%

2. Process Sequence*

   13.**AR Treat Superstrate Glass Deleted
   14. Mount Cells on Superstrate
   15. Cure Adhesive
   16. Apply Interconnects
   17. Apply Conformal Coat
   18. Cure Conformal Coat
   19. Mount in Frame
   20. Test Module

*Process sequence numbers continue from the cell area (Table 2.1)

**Steps where major modifications from original proposal have been introduced.

without back etching provided a suitable diffusion mask or edge clean-up process can be developed. Requirements for the aluminum firing have been further verified during this period.

At this point an additional printing and firing operation was introduced to locate dielectric isolation pads for the wrap-around contacts on the back aluminum. This was followed by printing solderable contacting pads on the back surface. During the second quarter silver contact pads on the aluminum back were found to be unsuitable because of galvanic corrosion effects. Tin applied by ultrasonic soldering techniques was found to be satisfactory. The front metallization grids and wraparound conductors are then printed. For this we originally proposed using an aluminum thick film paste. During the first quarter difficulties were encountered with aluminum front contact paste. It was decided to concentrate on developing a screen printed silver paste front contact process. Substantial progress has been made in understanding and improving the performance of screen printed silver front contacts.

2.2 TECHNICAL OVERVIEW OF MODULE DESIGN AND PROCESS SEQUENCE

The module design and selected process sequence are shown in Table 2.2. The module design is comprised of a 24 by 48 inch (60 x 120 cm) tempered glass superstrate. Square shaped cells were to be used in order to achieve 12% module efficiency goal. During the second quarter, square cells based on 3 inch diameter Czochralski crystals were decided on as test vehicles for process verification in anticipation of larger square or rectangular sheet materials becoming available. The crystals are to be shaped into prisms with square cross section prior to sawing wafers. The nominal wafer dimension will be 5.38 cm (2.12 inches) on the side. A tentative module design has been prepared comprised of a 10 x 20 cell layout. Cells will be interconnected into a

circuit with ten cells in parallel and twenty cells in series. The module is expected to have a peak power of 84 watts at 28°C and 9.4 volts.

The original proposal provided for formulation of an antireflection surface on the superstrate glass, using a sodium acid fluosilicate chemical treatment. After a preliminary evaluation of this process, we have concluded that it is not suitable as a low cost production process. An alternative process based on formation of silica from a water glass solution has been considered. It is not sufficiently developed for use on large structures and is deficient in performance and probably will be difficult to control as a production process. We have therefore decided to set this process step aside for the verification tests, although we consider AR treatment of the glass to be a desirable objective.

The module structure uses a thin bond line adhesive to attach the solar cells to the glass superstrate. Since silicone adhesives were known to be technically feasible, and the thin bond line minimizes costs, they were included in the original design. However alternative adhesives were to be evaluated in a search for greater cost effectiveness. A large number of adhesive candidates have been evaluated, and a final selection has not yet been made. Silicone adhesives are, however, still leading contenders. Interconnect conductors were to be in the form of thin copper foil mounted on a plastic film. The copper foil would be stamp-cut to preform the interconnects after mounting on the carrier film. A simple automatic reflow soldering operation is permitted by the wraparound techniques used to position both contacts on the back sides of the cells. After soldering, the carrier film and excess copper foil would be recycled. This scheme has been abandoned because of the costs of recycling the large fraction of material not actually used for

interconnects on any one module. Spool fed thin ribbons can be used with equal facility and without generating large amounts of recyclable scrap.

A silicone conformal coating was proposed as the encapsulant and rear surface, the module assembly to be completed by mounting the superstrate in an aluminum extrusion frame. A number of coating material candidates have been considered. Silicone is still a leading candidate, however acrylic and polyurethane candidates have been added for evaluation as possibly being more cost effective.

3.0 TECHNICAL DISCUSSION

3.1 DIFFUSION MASKING DIELECTRIC

3.1.1 Dielectric Formulation

Titania precipitated glasses (Series 5E) and baria-magnesia borosilicate glasses (Series 7E) have been selected as the most promising candidates diffusion masking dielectric[1]. The baria-magnesia series is of particular interest because it does not contain any alkali metal constitutents. Composition 7E-8-1A (with PbO added in the form of PbF_2 to improve adhesion[2]) was originally (and erroneously) believed to be too refractory.

During the present period a number of 7E series glasses were formulated (primarily varying the relative amounts of the B_2O_3 and Al_2O_3 constituents) with the goal of attaining a maturation temperature of 880°C. Compositions of the various formulation are given in Table 3.1.

The first of these compositions 7E-17 formed by adding 0.300 equivalents of Al_2O_3 to 7E-8-1A was far too refractory (no fusion at 950°C). Other variations in the composition of 7E-8-1A shown in Table 3.1 include:

1. Reduction in B_2O_3 content 7E-20 and 7E-21
2. Increase in MgO content 7E-22
3. Elimination of ZnO 7E-23
4. Increase in SiO_2 7E-24 and 7E-25

All coatings were blended with the screening vehicle using an alumina mortar and pestle. This procedure was followed to avoid iron contamination, which could be introduced by processing through the three-roll mill used heretofore. Additional variations were (1) the use of a platinum crucible for making some of the glass melts, and (2) zirconia instead of alumina grinding media in the ball mill for initial particle reduction of the glass frit.

Table 3.1

COMPOSITIONS OF SERIES 7E - MASKING DIELECTRICS

(Equivalents)

	7E-8-1A	7E-17	7E-18	7E-19	7E-20	7E-21	7E-22	7E-23	7E-24	7E-25
BaO	.253	.253	.253	.253	.253	.253	.204	.213	.253	.253
ZnO	.054	.054	.054	.054	.054	.054	.044	--	.054	.054
CaO	.054	.054	.054	.054	.054	.054	.044	.046	.054	.054
MgO	.612	.612	.612	.612	.612	.612	.687	.718	.612	.612
PbO	.027	.027	.027	.027	.027	.027	.022	.023	.027	.027
Total	1.000	1.000	1.000	1.000	1.000	.1000	1.001	1.001	1.000	1.000
B_2O_3	.492	.492	.492	.492	.450	.400	.397	.415	.491	.400
Al_2O_3	--	.300	.060	.075	--	--	--	--	--	--
SiO_2	.421	.421	.421	.421	.421	.421	.340	.355	.600	.421

Composition Changes to 7E-8-1-A

7E-17 Added 0.300 equivalents of Al_2O_3 for basic glass

7E-18 20 w/o 7E-17 and 80 w/o 7E-8-1-A

7E-19 25 w/o 7E-17 and 75 w/o 7E-8-1A

7E-20 Reduced B_2O_3 in 7E-8-1-A to 0.450 equivalents

7E-21 Reduced B_2O_3 in 7E-8-1-A to 0.400 equivalents

7E-22 Increased MgO in 7E-8-1-A to 0.850 equivalents

7E-23 Removed ZnO from 7E-22

7E-24 Increased SiO_2 in 7E-8-1-A to 0.600 equivalents

7E-25 Decreased B_2O_3 in 7E-24 to 0.400 equivalents

The use of zirconia grinding media exhibited a tendency to lower the maturation temperature of the coating. Smelts containing PbO, derived from PbF_2, turned black when melted in a platinum crucible. It was determined that the PbF_2 was reduced by the platinum.

The effects of the variations in composition and processing are summarized in Table 3.2. The most promising formulations are 7E-20 and 7E-24.

3.1.2 Diffusion Masking Dielectric, Cell Fabrication

Past attempts to fabricate solar cells using diffusion mask dielectrics have not been very successful[2]. The failure mode appeared to be bulk contamination of the silicon, causing a very low shunt resistance. This period we have attempted to produce cells using both diffusion mask dielectric and aluminum back surface field. Control cells were processed in parallel, in an attempt to determine the exact modes of failure. Table 3.3 defines the process sequence used to produce these cells. The first set of control wafers omitted Step 2 to determine whether the wafers might experience front surface contamination at this point. A second set of control wafers omitted Steps 2 and 3, to determine whether the presence of dielectric in the diffusion tube might create problems. Control cells required an edge clean-up which was provided by cutting 1.4" squares between Steps 9 and 10.

Five types of masking dielectrics (5E7, 5E7-1, 5E8, 7E20 and 7E24) were evaluated using this sequence. The results are given in Table 3.4. In every case cells with masking dielectric had a poor output as compared to the control cells. A number of cells from each group showed evidence of front silver contact peeling, which was attributed to poor cleaning procedures in Step 8.

Table 3.2

TEST RESULTS OF SERIES 7E

Composition	Crucible Material	Milling Media	Flow Characteristics			Maturing Temp. (°C)
			Temp (°C)	Time (Min)	Flow (mm)	
7E-8-1-A	Clay	Al_2O_3	900	7	46.5	800
	Pt	ZrO_2	800	7	42.0	750
			900	7	17.0	
7E-18	Clay	Al_2O_3	980	7	0	830
			880	7	17.0	
7E-19	Clay	Al_2O_3	980	7	22.0	830
			880	7	22.0	
7E-20	Clay	Al_2O_3	980	7	20.5	880
			880	7	33.0	
7E-21	Clay	Al_2O_3	980	7	0	880
			880	7	16.0	
7E-22	Pt	Al_2O_3	800	7	36.0	800
		ZrO_2	800	7	8.5	750
			900	7	0	
7E-23	Pt	Al_2O_3	800	7	25.0	800
		ZrO_2	800	7	21.5	800
			900	7	0	
7E-24	Clay	Al_2O_3	TBD			880
	Pt	Al_2O_3	TBD			800
7E-25	Clay	Al_2O_3	TBD			800
	Pt	Al_2O_3	TBD			800

Table 3.3

PROCESS SEQUENCE USED TO EVALUATE
DIFFUSION MASKING DIELECTRIC

1. Texture etch
2. Print and dry masking dielectric
3. Fire dielectric
4. Phosphine diffuse wafers
5. HF back of wafers
6. Print, dry and fire aluminum paste (Ampal 631 aluminum paste)
7. HF wafers
8. Remove unconsolidated aluminum powder and clean wafers
9. Print, dry and fire front silver paste

9a. Dice 1.4" squares (controls only)

10. Test cells

Control Set 1 omitted Step 2

Control Set 2 omitted Step 3

Table 3.4

RESULTS OF CELL FABRICATION TEST OF DIFFUSION MASKING DIELECTRICS

Sample	V_{oc} mV	I_{sc} mA/cm^2	I_{500} mA/cm^2	R_{sh} ohms
5E7-1	521 - 576	27.4 - 28.8	10.9 - 16.2	1.5 - 3.0
Control 1	600 - 603	29.9 - 31.1	19.1 - 25.5	11.3 - 12.6
Control 2	Cells Broke			
5E7	488 - 557	16.6 - 30.7	0 - 14.7	2.0 - 2.8
Control 1	591 - 604	30.6 - 31.5	21.4 - 26.0	8.1 - 33.1
Control 2	Cells Broke			
5E8	518 - 582	19.1 - 28.3	6.3 - 12.4	2.8 - 7.3
Control 1	598 - 603	31.2 - 31.9	18.8 - 25.9	18.1 - 104.1
Control 2	598 - 603	29.8 - 31.2	0 - 26.8	28.7 - 36.5
7E20	550 - 581	19.2 - 27.1	6.3 - 17.7	3.3 - 5.9
Control 1	599 - 606	31.4 - 31.5	22.5 - 27.0	15.1 - 33.1
Control 2	599 - 604	29.1 - 31.6	25.1 - 26.9	29.8 - 42.7
7E24	521 - 594	25.4 - 30.7	7.0 - 24.6	1.8 - 5.4
Control 1	600	31.7	26.1	36.8
Control 2	597 - 598	30.5 - 31.2	25.3 - 25.9	20 - 32.9

The 5 series dielectric had a low output at load, and portions of the aluminum back contact had peeled on the 5E7. This peeling of the aluminum contact occurs adjacent to the diffusion mask dielectric. Sanding the edges of the cells to improve output was not advantageous. Edge clean-up by sawing squares was not feasible with the diffusion dielectric, which fouled the dicing saw blade. The 7 series dielectrics divitrified and cracked during the diffusion step, which resulted in cells of low output. Sanding the edges of the cells improved the output, indicating that the 7 series dielectric is not an effective phosphine diffusion barrier. All of the cells produced with a dielectric had an erratic output at load which was attributed to high back contact resistance. This contact resistance was reduced by ultrasonically soldering tin pads to the back, opposite the front contact pads. Most of the cells showed a definite improvement in output, Table 3.5.

The results of this experiment indicate that diffusion mask dielectrics are detrimental to the cells' output and also have detrimental effects on the aluminum back surface field. Three of the dielectrics (5E7-1, 5E8 and 7E24) were then selected for further verification of these results. Cells were processed in accordance with the schedule shown in Table 3.1, except for an additional cleaning in a dilute solution of acetic acid at Step 8. These cells did not experience any front silver contact peeling, but did experience aluminum peeling associated with shear failure of the silicon. These cells had a reasonably high short circuit current (I_{sc} above 600 mA), but low open circuit voltage (V_{oc}) and output at load (I_{500}), Table 3.6. The application of the tin solder pad did not produce any noticeable improvement. These cells were subsequently edge etched, which improved the short circuit current, open circuit voltage and output at load. The dark reverse current at 500 mV was measured in order to estimate shunt resistance (R_{sh}). The shunt resistance for all the cells was too low (1-4 Ω) for good solar cell performance.

Table 3.5

EFFECT OF TIN SOLDER PAD ON CURRENT OUTPUT AT LOAD POINT, DIFFUSION DIELECTRIC TEST 2.12 INCH ROUND CELLS, NO AR COATING

Sample	I_{500} (mA) Al Contact	Sn Solder Pad
5E7-1	326	370
	315	348
	247	248
5E7	204	237
	61	83
	67	-0-
	61	105
5E8	130	243
	113	283
	-0-	171
	58	144
7E20	315	403
	124	146
	200	227
	274	334
	148	144
7E24	159	35
	-0-	Broken
	317	419
	298	381
	490	509
	400	560*
	364	547*

*Cell edge sanded

Table 3.6

AVERAGE VALUES OF PARAMETERS OF 2.12" ROUND CELLS FABRICATED WITH VARIOUS DIFFUSION DIELECTRICS

Dielectric	N	As Fabricated			After Edge Etch			
		V_{oc} mV	I_{sc} mA	I_{500} mA	V_{oc} mV	I_{sc} mA	I_{500} mA	R_{sh} ohms
5E7-1	9	558.2	648.0	194.0	584.0	660.4	406.8	2.89
5E8	8	534.8	641.8	96.6	577.2	667.6	345.6	2.09
7E24	5/4	531.6	615.2	74.8	571.0	632.2	265.8	1.83

It can be concluded from these experiments that: 1) The dielectrics are not a sufficient barrier to electrical conduction because of either conduction under, through or over the dielectric; 2) The silicon-dielectric interaction introduces detrimental effects into the bulk silicon which cause a low shunt resistance; 3) The aluminum-dielectric interaction causes peeling of the back aluminum-silicon contact possibly by interfering with the regrowth of the back surface field; 4) Some of the dielectrics studied react with the phosphine diffusion agent which causes the dielectric to divitrify. The extent of the problems associated with the dielectrics are too great to be solved within the time schedule of this contract. It is recommended that the diffusion mask dielectric be abandoned. For purposes of the verification run, some form of edge clean-up followed by application of a wraparound dielectric will be substituted for the diffusion mask.

3.2 ALUMINUM METALLIZATION

Efforts continued during July to find sources of junction shunting which have been interfering with the screen printing process. Damage to the tetrahedral peaks of the textured surfaces and aluminum contamination of the front surface and junction edge have been identified as causes of shunting. Near the end of the month a malfunction discovered in one of the screen printers was found to be a major source of severe shunting degradation of cells.

The time-temperature response surface for the aluminum firing process was explored further using paste made with Alcoa 1401 powder. In order to avoid confusion with problems arising from other causes, the following process sequence was devised for these experiments:

1) Texture etch wafers
2) Phosphine diffuse to 30 Ω/□
3) Back etch with 100% HF

4) Print, dry and fire aluminum paste
5) 10% HF for 2 minutes
6) Sand edge of wafer
7) Remove sintered (unmelted aluminum)
8) Clean wafers in acetic acid and solvents
9) Print, dry and fire silver front paste
10) Test cells

The sixth step of sanding the edge is a very unreliable process. If the edges are not sanded enough, shunting around the edge will remain, and if edges are sanded too much, wafer damage will occur, and will appear in the form of shunting. As one sands the edge of the wafer, the V_{oc}, I_{sc} and I at load will increase to a maximum and then decrease.

The results of a time and temperature matrix for 2.12 inch round cells processed by this sequence is given in Table 3.7. All of the cells that were fired at 900°C, except for the one fired for 10 seconds, had puddles of thick aluminum on the back, and the sintered (unmelted) aluminum was difficult to remove. The cells fired at 850°C had a good uniform layer of melted aluminum on the back.

The cells that had a uniform melted aluminum layer remaining on the back after the sintered aluminum was removed, and had the highest efficiency, were the ones fired at 850°C for 20 seconds. Cells fired at 750°C did not show any current at the 500 mV load point, consistent with the lack of an ohmic back contact. This was also true for the cells fired at 800°C for 20 and 30 seconds.

In order to estimate the extent to which the relatively low shunt resistance reported in Table 3.7 are attributable to edge effects caused by the edge grinding step, square cells 1.4 inches on the side were cut from the round cells. The results of this treatment are reported in Table 3.8. The shunt resistance in these square cells would be increased from the round cell by a factor of 1.8 to account

Table 3.7

Results of time-temperature firing cycle matrix for aluminum paste made with 70% Alcoa 1401 aluminum powder with 30% V-13 vehicle, 2.12 inch round cells with no AR coating.

Firing Time	750°C	800°C	850°C	900°C
		V_{oc} (mV)		
10 Sec.	--	--	607.5	610(1)*
20 Sec.	--	599	609	605(1)
30 Sec.	--	560	607.5	596(1)
40 Sec.	601.5	607.5	607	590(1)
50 Sec.	576	604	--	--
		I_{sc} (mA)		
10 Sec.	--	--	684	709(1)
20 Sec.	--	710	607.5	669(1)
30 Sec.		809.5	703	671(1)
40 Sec.	601.5	695	685	660(1)
50 Sec.	576.5	692.5	--	--
60 Sec.	566	--	--	--

Table 3.7 (continued)

Firing Time	750°C	800°C	850°C	900°C
		I_{500} (mA)		
10 Sec.	--	--	575.5	612(1)
20 Sec.	--	-0-	604	578(1)
30 Sec.	--	-0-	589.5	505(1)
40 Sec.	530	613.5	572	487(1)
50 Sec.	-0-	190(1)	--	--
60 Sec.	--	--	9.9	10.2(1)
		R_{SH} (ohms)		
10 Sec.	--	--	9.9	10.2(1)
20 Sec.	--	35.9	17.7	9.1
30 Sec.	--	33.2	7.6	4.2(1)
40 Sec.	9.6	25.2	14.6	5.7(1)
50 Sec.	13.5	29.2	--	--
60 Sec.	34.0	--	--	--

*Data are averages of 2 cells except where indicated otherwise. Complete data are given in Appendix A.

Table 3.8

EFFECT OF EDGE CONDITIONS ON SHUNT RESISTANCE
R_{sh}-Ohms

Firing Cycle	Round	Adj. for Size	Square	Change
900°C				
10 Sec.	10.2	18.4	57.5	39.1
20 Sec.	7.9	14.2	18.9	4.0
	10.2	18.4	23.7	5.4
30 Sec.	4.2	7.6	9.4	1.8
40 Sec.	5.7	10.3	12.1	1.8
800°C				
10 Sec.	9.4	16.9	27.0	10.1
	10.4	18.7	45.9	27.2
20 Sec.	16.7	30.1	51.0	20.9
	14.7	26.5	41.3	14.8
30 Sec.	8.6	15.5	46.7	31.2
	6.6	11.9	15.4	3.5
40 Sec.	18.5	33.3	53.8	20.5
	10.6	19.1	27.8	8.7
800°C				
20 Sec.	38.5	69.3	250	180.7
	33.5	60.3	57.5	-2.8
30 Sec.	20.8	37.4	185	147.6
	45.5	81.9	167	85.1
40 Sec.	31.3	56.3	75.8	19.5
	19.2	34.6	86.2	51.6
50 Sec.	41.7	75.1	89.3	14.2
	16.7	30.1	122	91.9

for the area differences. Examination of Table 3.8 indicates that some improvement resulted. It was relatively slight in about one third of the cases. In another third of the cases, improvement by a factor of two or more occurred.

In order to verify the efficacy of the 850°C - 20 second firing cycle, 10 cells were processed by the previously defined process sequence. Table 3.9 gives the results of this run, in which the average cell efficiency was 13.5%.

Atomized Metal Powder, Inc. (AMPAL) produces an aluminum powder (#631) having similar specifications to that of Alcoa 1401 (Alcoa 1401 is no longer available). A time temperature matrix was run on a paste prepared with this AMPAL powder (Table 3.10, set I). These cells were processed with the sequence of Table 3.3 eliminating the dielectric steps (2.12 inch rounds cut into 1.4 in. x 1.4 in. squares). The results of this matrix indicate an optimum firing temperature of 825°C for 30 to 50 seconds. This matrix was verified with a second experiment also reported in Table 3.10 (Set II). A problem associated with the screen printing of the front contact grids introduced a greater than normal variation in cell performance. It is evident from these experiments that longer firing times and higher firing temperatures are detrimental to shunt resistance, although it may not be evident from cell efficiency.

3.3 ISOLATION DIELECTRIC

The effort during this reporting period was concentrated on reducing the maturation temperature of the 6I2-2 (isolation) glass. This composition has a maturation temperature of 700°C. Compositions of experimental glasses which were evaluated are given in Table 3.11.

Table 3.9

PERFORMANCE OF ALUMINUM BACK SURFACE CELLS FIRED AT 850°C FOR 20 SECONDS
ALCOA 1401 ALUMINUM POWDER

AM1 28°C

V_{oc}	I_{sc}	I_{500}	R_{SH}	$\eta_{500\ mV}$
607	686	597	15.9	13.1
609	707	623	21.7	13.7
607	696	605	12.2	13.3
608	705	626	21.7	13.7
607*	701*	561*	5.2*	12.3*
608	702	614	20.0	13.5
610	699	607	15.6	13.3
610	712	615	16.1	13.5
611	709	623	20.0	13.7
609	705	613	17.9	13.5
Average:				
608.8	702.3	613.7	17.9	13.48

*Outliner data not included in statistical calculations.

Table 3.10

Time-temperature matrix for 1.4 inch square cells made with 70% Ampal #631 aluminum powder in 30% V-13 vehicle. Data reported are average of 5 cells. No AR coating on cells.

	Set I		Set II	
Firing Time	825°C	850°C	825°C	850°C
	V_{oc} (mV)			
20 Sec.	--	606.8	--	602.0
30 Sec.	608.8	606.4	602.8	601.5
40 Sec.	--	--	604.0	--
50 Sec.	606.8	--	601.3	--
	I_{sc} (mA)			
20 Sec.	--	398.8	--	393.0
30 Sec.	411.3	394.0	391.0	394.3
40 Sec.	--	--	392.5	--
50 Sec.	408.2	--	390.0	--

Table 3.10 (continued)

	Set I		Set II	
Firing Time	825°C	850°C	825°C	850°C
	I_{500} (mA)			
20 Sec.	--	307.6	--	322.0
30 Sec.	320.5	207	331.3	322.3
40 Sec.	--	--	335.0	--
50 Sec.	308.8	--	313.5	--
	η_{500} mV			
20 Sec.	--	12.2	--	12.7
30 Sec.	12.7	11.7	13.1	12.7
40 Sec.	--	--	13.2	--
50 Sec.	12.2	--	12.4	--

Table 3.11

COMPOSITION OF SERIES 6 ISOLATION GLASSES

Oxide	6I2-2-A	612-8	612-9	612-10
Li_2O	0.605	0.605	0.605	1.000
ZnO	0.395	0.395	0.395	---
Total	1.000	1.000	1.000	1.000
B_2O_3	4.608	4.795	4.795	7.926
Al_2O_3	0.186	---	---	---
Ta_2O_5	0.096	0.096	---	---
SiO_2	1.395	1.395	1.395	2.306

The first modification, 6I2-2-A retained the same composition as 6I2-2 but derived the Li_2O from Li_2CO_3 instead of from LiF. The maturation temperature for this coating was 650°C. Maturation temperatures for the other glass were all above 650°.

Fusion flow measurements which have been made for Series 6 glasses are reported in Table 3.12.

3.4 BONDING AND BACK COATING MATERIALS

The current status of candidate materials which have been considered for cell-to-superstrate bonding and for module back coating are reviewed in Tables 3.13 and 3.14, respectively.

Changes from previous reports include addition of DuPont Elvax 150 ethylene vinyl acetate and Advanced Coatings and Chemicals Urafilm 1-1C-5 polyurethane to the list of candidates backside protective coating materials, and the elimination of Photo Chemical Products Perma Resin, and Deft Chemical Coatings MIL-L-81352 Acrylic Lacquer. The ethylene vinyl acetate was added on the basis of low cost and very promising reports on the material for use in such applications. The elemination of Perma Resin was based on deterioration of adhesion under humidity exposure, and the MIL-L-81352, because of generally poor adhesion.

Ethylene vinyl acetate is also potentially applicable for use as an adhesive for cell to superstrate bonding, but the protective coating application will be evaluated first. Use as an adhesive would involve hot melt application which is a significant deviation from presently planned bonding processes.

Table 3.12

FLOW CHARACTERISTICS OF 6I2 SERIES

Coating	Milling Condition	Time (Min.) Hor.	Time (Min.) Vert.	Temp. (^{o}C)	Flow (mm)
6I2-2	Wet	1½	4	750	23.2*
6I2-2	Dry	1½	4	700	34.5
6I2-2	Dry	1½	4	750	Excessive
6I2-3	Wet	1½	4	700	24.5*
6I2-3	Dry	1½	4	750	28.0*
6I2-5	Wet	1½	4	750	Excessive
6I2-6	Wet	1½	4	750	22.5*
6I2-7	Wet	1½	4	700	22.0*
6I2-7	Wet	1½	4	750	21.5*
6I2-8	Dry	1½	4	700	41.5
6I2-8	Dry	1½	4	750	

*Bubbles

Table 3.13

STATUS OF CANDIDATE ADHESIVE MATERIALS

MANUFACTURER	IDENTIFICATION	TYPE	COMMENTS
Retained for further consideration:			
General Electric	RTV 615	Silicon RTV	
Dow Corning	96-083	Silicone Adhesive	
General Electric	RTV 2144-131	Silicon RTV	
Eliminated:			
Dow Corning	Q1-2577 (mica)	Silicon B Stage	Poor light transmission
Dennison	Densil tape	Double Backed	Bubbles and unbonded areas
Loctite	Loctite 524/525	Acrylic/accelerator	Poor light transmission
Hughson	Versilock 506/4	Acrylic/accelerator	Poor light transmission
Hughson	Versilock 521/4	Acrylic/accelerator	Poor light transmission
Franklin	Rexite P2/SB	Acrylic/accelerator	Poor light transmission
Hysol	EA9446/AB	Acrylic/accelerator	Poor light transmission
Ciba-Geigy	DA-560-4	Acrylic UV Cure	Poor temperature resistance
Rhom and Haas	Acryloid B-7	Acrylic, Thermo-plastic	Bubbles and unbonded areas, poor temperature resistance
Dow Corning	X3-6558	Silicone gel	Poor adhesion and permanently soft, tacky surface
Loctite	353	Acrylic UV cure	Loss of transmission λ <1000m μ after UV exposure
Loctite	524	Acrylic heat cure	Loss of transmission λ <700m μ after UV exposure
Shell	Epon 828/Versanid 125	Epoxy	Loss of transmission λ <550m μ after UV exposure

Table 3.14

STATUS OF CANDIDATE PROTECTIVE COATING MATERIALS

MANUFACTURER	IDENTIFICATION	TYPE	COMMENTS
Retained for Further Consideration:			
Dow Corning	Q1-2577	Silicone Coating	
Dow Corning	X3-5053	Silicone Emulsion	
Contour Chec. Co.	XB-1786	Silicone Coating	
Product Techniques	PT 469 Clear	Modified Acrylic	
Bostic Finch	MIL-C-83286	Polyurethane	
Rustoleum	C-1590 white	Alkyd	
DuPont	Elvax 150	Ethylene Vinyl Acetate	
Advanced	Urafilm 1-1c-5	Polyurethane	
Eliminated:			
General Electric	RTV 615	Silicone	Poor adhesion
Rohm & Haas/ Mobay	QR-568/ Desmodure N75	Oxazolidine Acrylic Polyurethane	Delamination during thermal cycle
Rohm & Haas	Acryloid B-7	Acrylic	Poor adhesion
Dow Corning	R-4-3117	Silicone Coating	Poor adhesion
Photo Chem Prod.	Perma Resin	Epoxy-Acrylic	Poor adhesion after humidity exposure
Deft Chem. Coat.	MIL-L-81352	Acrylic	Poor adhesion

Table 3.15 reviews the results of adhesion-environmental exposure tests made to date on candidate protective coating materials on MIL-L-81352 acrylic lacquer, Product Technique PT 469 white, Rustoleum C-1590 white alkyd and MIL-C-83286 polyurethane with Chemlok AP-131 primer, Dupont Elvax 150 and Advanced Coating and Chemicals Urafilm 1-1C-5.

Peel strength entries shown as >2 represent coating materials with peel strengths too high to be measured by this method. This includes any material with properties such that its peel strength is greater than the apparent strength of the fiberglass cloth backing which is used to apply the peeling stress to the coating. However, this apparent strength of the fiberglass varies over a wide range. The lower part of the range appears to result from stiffening of the fiberglass cloth by impregnation with the coating materials. With the higher modulus coatings this causes flectural fracture at loads very much below those for normal tensile failures of unstiffened fiberglass. Therefore the method tends to be invalid for the higher modulus coating materials. The >2 reported for these peel strengths is somewhat arbitrary, but on the basis of supplemental observation, scraping, tape pull tests, etc., 2 lbs/in. appears to be a reasonable minimum for the materials involved.

In order to obtain more definite peel strength values, a modified procedure was used in which a flexible adhesive was used to bond a second strip of heavier fiberglass on top of the original. PR 1201Q polysulfide adhesive was used for this purpose. Then the two fiberglass layers were pulled simultaneously. The results of these tests are shown in Table 3.16. In some cases the original fiberglass still could not be peeled without breaking. These are indicated by ">" symbols in front of the corresponding data. These ">" values represent the peel strength of the polysulfide adhesive against the corresponding coating material. Although generally higher than the apparent strengths of the original fiberglass

Table 3.15

COATING MATERIALS EXPOSURE/ADHESION TESTS

Material	Peel Strength Tests (Pound/inch) (Average Apprcx. 10 Specimens)						Tape Adhesion Test % Area Failed			
	Cured Film Control		Thermal Cycle -40° to 100°C		Humidity 95% 70°C		Coating as cured		H_2O 24 Hrs Immersion	
	Cell	Glass	Cell	Glass	Cell	Glass	Cell	Glass	Cell	Glass
Q1-2577	0.6	0.2	0.6	0.2	0.2	0.1	100	100		
R4-3117	1.3	0.1	1.1	0.1	1.2	0.1	100	100		
X3-5035	1.7	1.8	1.9	1.9	1.1	1.0				
MIL-C-83286	3.64	1.84	3.38	1.02	1.62	1.69	Pass	Pass	Pass	100
MIL-L-81352	.645	.08	1.06	.009	.52	.37	50	50	100	100
XB-1786 (w/primer)		1.4*								
C-1590 white		2.5*								
PT469 clear	>2	>2	>2	>2	>2	>2	Pass	Pass	Pass	100%**
PT469 white	>2	>2	>2	>2	>2	>2				
Perma Resin	>2	>2	>2	>2	>2	.49	Pass	Pass	Pass	100%
MIL-C-83268 with AP-131 Primer	>2	2.5	>2	2.4	>2	>2				
ELVAX 150		2.8								
Urafilm 1-1c-5	>2	2.8	>2		>2					

*Less than 10 specimens
**Passed if coating baked 40 minutes. Failed with 15 minute bake.

Table 3.16

COATING MATERIALS EXPOSURE/ADHESION TESTS

	Modified Peel Strength Tests (Pound/inch) (Average 2 Specimens)					
	Cured Film Control		Thermal Cycle -40°C to 100°C		Humidity 95% 70°C	
Material	Cell	Glass	Cell	Glass	Cell	Glass
PT469 Clear	3.7	>1.88	>2.15	>3.35	>1.98	>1.88
PT469 White	>1.8	>2.1	>1.8	>1.45	>1.05	> .58
Perma Resin	1.98	>2.15	1.65	>1.05	.90	.06
MIL-C-83286 with AP-131 Primer	3.5	2.4	4.1	3.7	4.4	5.0

backings, these values obviously are not as high as the true peel strength of the corresponding coatings. Also, the scatter is too great to establish a definitive minimum.

Table 3.17 reviews the bond strength-environmental exposure tests made to date on candidate adhesive materials. In addition to previously reported data, this includes test results on Dow Corning 96-083 self priming silicone adhesive, and General Electric 2144-131 RTV silicone, the latter both with and without a primer.

Recent developments in protective coating technology have been focusing on the immediate interfacial surfaces between coatings and substrates. This can involve the use of various types of coupling agents whether as additives to coating materials or as primers to promote molecular bonding of the coating to all available sites on the opposite surface. The intent is to create an interface so intimately bonded that any contaminant permeating the coating will have no sites to chemically interact with the surface.

The effect of a swelling solvent on coated specimens is the basis of one test to evaluate this resistance of interfacial bonds to permeating species. In order to evaluate the method, several different silicone primer systems were used in the application of RTV 615 silicone coatings to solar cell surfaces. These specimens were then immersed in xylene to swell the silicone coating, and the time required for any visible wrinkling or lifting was observed. A similar test was made using Sylgard 184 silicone. Results are reported in Table 3-18. Several other coating materials have been tested for permeation and lifting in a somewhat similar manner by exposure to boiling deionized water. The results in Table 3.19 show the times of exposure required for significant loss of peel strength. The significance of this relative to real time weatherability of the coatings is not immediately evident. However it does very quickly show distinct differences and should be effective at least as a screening test for distinguishing between materials.

Table 3.17

BOND STRENGTH/EXPOSURE

LAP SHEAR STRENGTHS LBS/IN^2

(AVERAGE APPROX. 10 SPECIMENS)

MATERIAL	AS BONDED, CONTROL			THERMAL CYCLE -40°C to 90°C			HUMIDITY @ 70°C		
	CELL TO CELL	CELL TO GLASS	GLASS TO GLASS	CELL TO CELL	CELL TO GLASS	GLASS TO GLASS	CELL TO CELL	CELL TO GLASS	GLASS
RTV 615	145		173	86		191	250		218
RTV 615/4120 Prim	330		250	195		238	310		264
RTV 615/4155 Prim			205			234			266
RTV 615/1204 Prim		56.5			121			57.0	
RTV 615/Sylgard Prim		290			473			420	
X3-6558	7.5		123	8.5		125	12.3		161
Loctite 524	812		448	566		428	369		280
Epon 823/Vers 125	744	740	284	272	764	273	436		278
Loctite 353 U.V.		527	572		766	591	468		453
96-083	474			540			423		
GE 2144-131	79			77			100		
GE144-131/4120	108			122			145		

Table 3.18

RESISTANCE OF SILICONE ELASTOMERS TO SWELLING IN XYLENE

PRIMER COUPLING TESTS

	1st Detectable Lifting	
Primer	RTV 615	Sylgard 184
SS 4155	10 min.	30 min.
SS 4120		2 min.
Q3-6060	10 min.	10 min.
1204	2 min.	2 min.
Sylgard	2 min.	2 min.
Piccotex	1 min.	1 min.

Table 3.19

COATING MATERIALS BOILING WATER RESISTANCE

TIME (sec) TO SIGNIFICANT LOSS OF PEEL STRENGTH

	Substrate	
Coating Material	Cell	Glass
MIL-C-83286		10
MIL-C-83286/AP-131 Primer		240
Urafilm	180	
Perma Resin		10
PT469		300

3.5 THERMAL STRESSES IN BONDED SOLAR CELL PANELS

Thermal stress was investigated by subjecting test specimens to cycling from 100°C to progressively lower temperatures to determine the temperature at which differential thermal expansion reached a damaging level. Test specimens consisted of two interconnected 3" solar cells bonded to a glass panel. Bonding materials used include RTV 615 Silicone, 96-083 silicone, and Epon 828/Versamid 125. The same cure temperature, 150°C, was used for all specimens. Specimens were examined for any evidence of damage after each successive low temperature exposure, and also solar cell electrical output measurements were made before and after each cycle.

The low temperature extreme tested to date was -80°C. At this point electrical output has been virtually unaffected, and no detectable mechanical damage has occurred. The one detectable effect is a slight yellowing of the Epon 828/Versamid 125 adhesive.

3.6 SUPERSTRATE AR COATING

An evaluation was made of the acid etch process for forming an antireflective coating on glass. This process uses a silica supersaturated solution of fluosilicic acid to selectively dissolve the metal components in the glass[3]. The result is a thin layer of skeletonized pure SiO_2. Due to its porous nature this layer has a low refractive index and can act as an AR film. The selective etching properties of the acid solution depend critically on the silica supersaturation, an essentially unstable condition. We do not believe this process will be an effective, controllable production process because of the solution instability.

Another process for forming antireflective coatings on glass is the development of an SiO_2 layer by acid hardening of a film of sodium silicate (water glass) in aqueous solution. This process

has been investigated by Motorola[4]. In their work the sodium silicate solution was applied by photoresist spinning techniques. The films produced were less effective than acid etched films, with peak transmission losses of approximately 1% per side.

We have evaluated coatings formed from water glass films applied by dipping into the solution and, in general, verified the Motorola observations regarding transmission. We have also observed that effectiveness of the coatings is strongly dependent on thickness and uniformity. We have concluded that the process is not adequately developed to handle large panes of glass, moreover the effectiveness leaves something to be desired.

Because of these considerations, we have decided to delete this step in the process sequence for the present. However we consider that the potential improvement in module efficiency is so great that further efforts should be made to develop a suitable process. Reflective losses from glass cover panes amount to about 4%. Assuming a module price of $0.50 per watt a module efficiency of 12%, elimination of this loss would be worth about $2.40 per square meter. Elimination of the loss for a cost less than this would be cost effective.

3.7 ASSISTANCE TO LOCKHEED

Assistance was provided to Lockheed, Inc. on the processing of aluminum back contacts for their LSA Task IV contract. This assistance consisted of printing and firing a number of wafers and suggesting possible causes of problems after reviewing their process.

4.0 CONCLUSIONS

4.1 A malfunctioning screen printer was identified as a major cause of shunt resistance problems. Aluminum contamination of the junction edge is a secondary source of low shunt secondary source of low shunt resistance. Excessive firing time and temperature also contribute to reduced shunt resistance.

4.2 Aluminum screen printing pastes made with different aluminum metal powders require different time-temperature firing cycles for optimum results.

4.3 The diffusion mask process as we are presently practicing it is not a viable process.

4.4 The acid etching and sodium silicate processes for forming antireflective surfaces on glass are not adequately developed for processing large panes of glass. The former process is not suitable for mass production due to control difficulties arising from the use of a supersaturated solution. The latter process is difficult to control and is not completely effective.

5.0 RECOMMENDATIONS

5.1 It is recommended that verification testing be commenced with the following alterations in the originally proposed process sequence:

1) Elimination of the diffusion mask process.

2) Separate firing cycles for the diffusion and aluminum back contact.

3) Removal of the diffusion oxide.

4) Use of an edge clean-up process in lieu of the diffusion mask.

5) Wraparound of the isolation dielectric in lieu of diffusion masking dielectrics.

6) Use of silver screen printed paste for front metallization instead of aluminum.

7) Application of a tin pad on the aluminum back instead of a silver pad for making soldered interconnect contacts.

8) Use of evaporated SiO AR coating in lieu of retaining the diffusion oxide.

9) Elimination of the AR coating on the glass superstrate.

Of these changes, the methods to be used for Items 3, 4, and 8 are for the purpose of conducting the verification experiments, and are not intended to be recommendations for long-term incorporation in the process sequence. Item 9 is to be regarded as a temporary expedient, not as a permanent change in the process sequence.

6.0 REFERENCES

(1) W. Taylor, W. Kimberly, N. Mardesich and A. Pepe, "Array Automated Assembly, Phase 2", (Spectrolab, Inc., Sylmar, California) JPL Contract 954853, Quarterly Report (May, 1978), DOE/JPL 954853-78/2.

(2) W. Taylor, W. Kimberly, N. Mardesich and A. Pepe, "Array Automated Assembly, Phase 2", (Spectrolab, Inc., Sylmar, California) JPL Contract 954853, Quarterly Report (August, 1978), DOE/JPL 954853-78/2.

(3) R. E. Peterson and J. W. Ramsey, "Thin Film Coatings in Solar-Thermal Power Systems", Jl. Vac. Sci. Technol., 12(5), 1023-1031, 1975.

(4) E. Pastinik, T. Sparks, and M. Coleman, "Studies and Testing of Antireflective Coatings for Soda Lime Glass", (Motorola, Inc., Phoenix, Arizona), JPL Contract 954773, Final Report, (January, 1978).

*U.S. GOVERNMENT PRINTING OFFICE: 1979-640-014/4448. Region 4.